



Comparison of edge discrimination of microbubbles between Sobel and improved mathematics of Canny edge detection

Ayman S. Qaddoori^{a,*}, Jamila H. Saud^b

^aInformatics Institute for Postgraduate Studies Iraqi Commission for Computer and Informatics, Baghdad, Iraq

^bCollege of Science, Mustansiriyah University, Baghdad, Iraq

(Communicated by Madjid Eshaghi Gordji)

Abstract

Bubble sizes are generated by micro-bubble generators (MBGs) in the water for their effect on the percentage of dissolved oxygen in the water and we find this in aquaculture where oxygen is important to marine life and in many applications. And since these bubbles range in size from 20 to 50, we need to highlight the shape of the bubble and distinguish it, so two Sobel algorithms were used and the Canny method was improved and compared between them, where the edge detection algorithm is sensitive to noise, and therefore, it is easy to lose weak edge information when filtering noise, and it appears its fixed parameters are weak adaptability. In response to these problems, this paper proposed an improved algorithm based on the Canny algorithm. This algorithm introduced the concept of gravitational field strength to replace the image gradient and obtained the gravitational field strength factor. Two methods for choosing the adaptive threshold based on the average image gradation. The size and standard deviation of two types of model images (one containing less edge information, the other containing rich edge information) were subtracted, respectively. The improved Canny algorithm is simple and easy to achieve. Experimental results show that the algorithm can retain more useful information and is more robust in the face of noise.

Keywords: Bubble size, Detection Technique, Sobel edge detection, improved Canny algorithm.

*Corresponding author

Email addresses: ms201910470@iips.icci.edu.iq (Ayman S. Qaddoori),
dr.jameelahharbi@uomustansiriyah.edu.iq (Jamila H. Saud)

Received: August 2021 Accepted: September 2021

1. Introduction

Image edge information, which can define the target shape, relative position within the target region, and other essential information, is one of the most significant pieces of information in an image. One of the most essential processes in image processing is edge detection, which has a direct impact on picture interpretation. The highest value of the first derivative or the zero crossing of the second derivative are used in classic edge identification algorithms [13]. Although representative first order differential operators (Roberts operator, Prewitt operator, Sobel operator, and so on) and second order differential operators (Laplace operator, LOG operator, and so on) have many advantages such as simple computation, rapid speed, and ease of implementation, they are more sensitive to noise and their detection effect in engineering applications is not perfect [3]. The Sobel Operator, also known as the Sobel – Feldman operator or the Sobel filter, is used in image processing and computer vision, particularly in edge detection, when the picture is emphasized by edges. It was named after Irwin Sobel and Gary Feldman, two Stanford Artificial Intelligence Laboratory (SAIL) colleagues. Sobel and Feldman proposed the notion of the "Isotropic 3×3 Gradient Operator" at a presentation at SAIL in 1968. It's a sophisticated differentiation operator that gauges the gradient approximation of the picture intensity parameter in technical terms [12, 9].

Canny established three performance criteria for edge detection operators: SNR, localization precision, and single edge response, and determined the optimal Canny edge detection operator [8, 5]. In most situations, when compared to conventional edge detection algorithms, the Canny method outperforms them [1]. In recent years, several academics have proposed and implemented a number of enhanced algorithms based on the Canny algorithm to practical engineering. By using Otsu's threshold selection technique, ErSen Li enhanced the image gradient magnitude calculation operator and the automaticity of edge detection, and it exhibited good edge detection results to some extent [2, 7].

Because image quality is influenced by factors such as noise and illumination during the image acquisition process, and because the local contrast of images in a large view scope varies, the parameters of the traditional Canny edge detection algorithm are fixed and cannot adapt to the edge detection process in different conditions. As a result, this research enhanced the image gradient calculation operator, allowing for more relevant detail edges to be preserved while also being more noise resistant. Two adaptive threshold selection approaches were provided for two types of typical images, and they can help to automatically suit different circumstances [?].

2. Background Theory

2.1. Sobel Operators

As mentioned previously, a way to avoid having the gradient calculated about an interpolated point between pixels is to use a 3×3 neighborhood for the gradient calculations. Consider the arrangement of pixels about the pixel $[i,j]$. The Sobel operators is the magnitude of the gradient computed by [4]:

$$M = \sqrt{S_x^2 + S_y^2} \quad (2.1)$$

Where the partial derivatives are computed by:

$$S_x = (a_2 + ca_3 + a_4) - (a_0 + ca_7 + a_6) \quad (2.2)$$

$$S_y = (a_0 + ca_1 + a_2) - (a_6 + ca_5 + a_4) \quad (2.3)$$

With the constant $c = 2$. Like the other gradient operators, S_x and S_y can be implemented using convolution masks:

$$S_x = \begin{bmatrix} -1 & 0 & 1 \\ -2 & 0 & 2 \\ -1 & 0 & 1 \end{bmatrix} \quad S_y = \begin{bmatrix} 1 & 2 & 1 \\ 0 & 0 & 0 \\ -1 & -2 & -1 \end{bmatrix}$$

Note that this operator emphasizes pixels that are closer to the center of the mask. Sobel operators are one of the most commonly used edge detectors [10].

2.2. Canny Edge Detection

These approaches have several phases, each step is discussed in further depth in order to extract the edges precisely:

2.2.1. Image Filtering

The initial step toward smoothing the image in a typical Canny algorithm. In addition to the best approach of the optimum rim detection operator, Canny deducted the first derivative of the Gaussian function. To smooth the image according to row and column choose the suitable 1-D Gaussian function: i.e. perform converting operation into an image matrix. As the operation of convolution compliant commutative law and associative law, Canny method usually employs a Gaussian function of two dimensions to smooth the image and remove the noise. Edge detection Canny is a multi-stage method which can simultaneously identify edges with noise suppressed.

$$G(x, y) = \exp [-(x^2 + y^2)/2\sigma^2] / 2\pi\sigma^2$$

where σ stands for the parameter of the Gaussian filter, and it controls the extend of smoothing image.

2.2.2. Image Gradient Calculation

The second step is the calculation of the image gradient magnitude and direction. In order to compute value and direction of the gradient, the classic Canny method employs a restricted difference of 22 nearby zones [11]. From these formulés, K may be obtained the first-order partial derivative approach on the X and Y axes.

$$E_x[i, j] = (I[i + 1, j] - I[i, j] + I[i + 1, j + 1] - I[i, j + 1]) / 2$$

$$E_y[i, j] = (I[i, j + 1] - I[i, j] + I[i + 1, j + 1] - I[i + 1, j]) / 2$$

Therefore, the templates of the image gradient calculation operator are:

$$G_x = \begin{bmatrix} 1 & 1 \\ -1 & 1 \end{bmatrix} \quad G_y = \begin{bmatrix} 1 & 1 \\ -1 & -1 \end{bmatrix}$$

Therefore, the templates of the image gradient calculation operator are:

$$\|M(i, j)\| = \sqrt{E_x[i, j]^2 + E_y[i, j]^2}$$

The azimuth of the image gradient i

$$\theta(i, j) = \arctan (E_y[i, j]/E_x[i, j])$$

2.2.3. Non-maximum Suppression (NMS)

After image magnitude gradient $M[i, j]$ has been obtained, non-maximum removal is necessary in order to place the edges properly. The NMS method may assure a one-pixel width for each edge. The Canny method employs 33 adjacent regions, which are composed of eight directions in order to perform interpolation in the direction of the gradient. If the $M[i, j]$ magnitude is more than the results of the two interpolations in the path, it shall be marked as the point at the end of the path, else it shall be marked as non-edge. Therefore, the image of the candidate edge is obtained.

2.2.4. Checking and Connecting Edges

The double-threshold algorithm Canny employs to choose edge points after non-maximum elimination. The pixels whose gradient size is beyond the high threshold must be marked as edge points, those whose gradient size is under the low threshold shall be tagged as pointless, and the remainder shall be recorded as edge points of the candidate. The edge points of the candidate that are connected to edge points are marked as edge points. This approach decreases the noise impact on the end edge of the image.

2.2.5. The Traditional Algorithm of Canny problems

Although the conventional method for the identification of Canny borders is utilized in more practice, there are two elements which may still be improved. The first is that in order to compute the image gradient, the standard method takes first order a restricted difference of 2 to 2 adjacent areas. It is easy to calculate, but it is more noise-sensitive. Due to the lack of a deviation in the 45° and 135° direction, actual edge data might be easily lost. The second is that there is a predetermined value for the double threshold for the classic Canny method. The flexibility of the classic Canny algorithm is not suitable for images with rich border information, and information about the local border can be easily lost. In that article, the gravity field intensity idea was presented to replace the gradient and the two adaptive techniques of selecting thresholds were proposed for two types of images.

2.3. Improved Canny Edge Detection

This method has been enhanced because of various difficulties in the old way of canny removal, which each step is detailed as indicated in the following:

2.3.1. Image Gradient Calculation

To compute the image gradient, Wang expanded the surrounding region 2×2 to 3×3 using the Sobel operator [14]. In order to make a change, Li utilized Prewitt operator [5]. The introduction of partial derivative of the diagonal direction retained further edge data and enhanced the accuracy of the edge location. Experimental results show that a larger-masked edge operator can offer a superior outcome. Sun has suggested a new edge sensor based on universal gravity theory which in this article is dubbed the algorithm of gravitational edge detection. Their performance on the edge of the individual criteria is not only better than those of Sobel and Prewitt, but also retains more valuable edge data and has a good noiset inhibitory effect. As Newton states in the law of universal gravitation, everything attracts each other by the force of its masses . The force between two bodies is given by:

$$\vec{F}_{1,2} = \frac{Gm_1m_2}{\|\vec{r}_{1,2}\|^2} \cdot \frac{\vec{r}_{1,2}}{\|\vec{r}_{1,2}\|}$$

G is a gravitational constant, G is a vector between body 1 and body 2 where m1 and m2 are the masses of the body. In the gravitational border identification technique, every pixel was supposed to

represent a bodily body of a mass equal to its gray value, the universal gravity law was applied to image processing. Therefore, it is possible to compute the Ftotal force which is the sum of various forces operating on the body. To do edge detection, Sun et al. used the F total. From above the performance of the method for gravitational edge identification in a bright zone or dark region can easily be found to be quite different. If a pixel in the dark zone (small gray value, low mass), when the pixel has the same gradient, the resulting gravitational force is less than that in the light zone. As a result, the gravitational method tends to make gradient changes in dark areas less important, leading to loss of edge points. This work therefore introduced the strength of the gravitational field to overcome the disparity between bright areas and dark areas. By following formula the intensity of the gravitational field may be calculated:

$$\vec{E} = \frac{Gm}{\|\vec{r}\|^2} \cdot \frac{\vec{r}}{\|\vec{r}\|}$$

Where G is a constant, m is the pixel’s mass (gray value). The resultant total intensity of the gravitational field is the combination of the intensity of gravitational field created by the pixels around the image. The resultant intensity of the gravitational field is regarded in this paper as an image gradient; the pixel is a border point when the intensity of the pixel is larger than the threshold. By using the following formula the total field intensity given to a spot may be calculated:

$$\vec{E}_{total} = \sum_{i=1}^n \frac{Gm_i}{\|\vec{r}_i\|^2} \cdot \frac{\vec{r}_i}{\|\vec{r}_i\|}$$

Pixels’ position in 2 x 2 neighboring areas. Assume that the distance between two horizontal or vertical pixels is 1, the distance between two diagonal pixels is 2, so the gravitational intensity on the point O in the 2 x 2 neighboring area (gravitational field intensity produced by pixels further away is negligible) can be calculated by the following formulas.

The gradient component on the X direction is:

$$\vec{E}_x = \sqrt{2}G (m[i + 1, j + 1] - m[i, j + 1] + m[i + 1, j] - m[i, j]) \vec{i}$$

and the gradient component on the Y direction is:

$$\vec{E}_y = \sqrt{2}G (m[i + 1, j + 1] - m[i + 1, j] + m[i, j + 1] - m[i, j]) \vec{j}$$

Therefore, the gradient magnitude is:

$$E = \sqrt{E_x[i, j]^2 + E_y[i, j]^2}$$

and the azimuth of gradient is:

$$\theta = \arctan (E_y/E_x)$$

Where \vec{i} and \vec{j} are the unit vectors on the horizontal and vertical direction respectively. ς is the direction of the gravitational field intensity. In practice, the G can be set to other value to act at some special circumstances. If let $G= 2/2$, it can be seen from (11) that the gravitational field intensity calculation template is the same to the traditional Canny gradient calculate operator for the 2 x 2 neighboring area. In order to retain more edge information, this work extend the neighboring area form 2 x 2 to 3 x 3 window. Table (1) shows the pixels’ position of 3 x 3 window.

Table 1: Pixels' Position

$I[i-1,j+1]$	$I[i,j+1]$	$I[i+1,j+1]$
$I[i-1,j]$	$I[i,j]$	$I[i+1,j]$
$I[i-1,j-1]$	$I[i,j-1]$	$I[i+1,j-1]$

Assume that the gray value of the pixel which is on the top left corner of the center pixel $I[i,j]$ is m_1 , and clockwise around it are m_2, m_3, \dots, m_8 . The Equation (2.14) can be applied to calculate the resulting total intensity of the center point.

The gradient component on the X direction is:

$$\vec{E}_y = G \left[(m_4 - m_8) + \sqrt{2}(m_5 - m_1 + m_3 - m_7)/4 \right] \vec{i}$$

and the gradient component on the Y direction is:

$$\vec{E}_x = G \left[(m_2 - m_6) + \sqrt{2}(m_1 - m_5 + m_3 - m_7)/4 \right] \vec{j}$$

Therefore, the gradient magnitude is:

$$\left\| \vec{E}(i, j) \right\| = \sqrt{\vec{E}_x[i, j]^2 + \vec{E}_y[i, j]^2}$$

and the azimuth of gradient is:

$$\theta = \arctan \left(\left\| \vec{E}_y[i, j] \right\| / \left\| \vec{E}_x[i, j] \right\| \right)$$

Make the constant $G=1$, it's easy to obtain the 3×3 neighboring area operator:

2.4. Adaptive Threshold Selection

Since the parameters of the original Canny algorithm were fixed, leading to the algorithm being unable to adjust to various conditions, two techniques of adaptive threshold selection for two types of typical images were introduced. In the edge detection procedure, the enhanced method can automatically obtain thresholds. The edge is the regions with a big variation in magnitude, i.e. the edge pixels are of a significant size. The histogram of the gradient can explain the edge intensity data. Two typical scenarios are present in practical engineering with the detection of image edge: (1) lower edge data, mostly in the microscopic field of vision; (2) a large field of view and rich border information, where the edge pixels are relatively larger and the contrasting local image is not uniform. After the image gradient has been obtained. In general, in the image, the edges only occupy a tiny proportion and hence the majority of pixels are non-edge pixels in the image gradient histogram within a limited gradient range. The size of the border pixel is huge and there is a fairly limited number of border pixels. With the rise in the gradient magnitude the number of pixels drops. In this article, two adaptive threshold selection techniques are available for these two common edge extraction images. The choice of threshold is very closely related to the mean gradient size and standard deviation. The medium of the gradient magnitude response and the default difference represent the discrete gradient magnitude distribution degree.

(1) Method for image with less edge information

The gradient magnitude of majority of the pixels is located in a small range in images with less

edge information. The mean of gradient magnitude and the standard deviation of this kind of images is small relatively. Images in the field of micro-vision always have less edge information. The distribution of the gradient magnitude of those non-edge pixels is concentrated, therefore, a proper double-threshold can help select edge pixels out. The double-threshold selection method for images with less edge information

where E_{ave} stands for the mean of gradient magnitude, m and n are the number of pixels on the image width direction and height direction respectively, $E[i, j]$ stands for the image gradient magnitude, i.e., the gravitational field intensity, T_h and T_l stand for high threshold and low threshold respectively, σ is image standard deviation, and k is its coefficient. The value range of k can be obtained through experiment, and $k \in (1.2, 1.6)$. When image edge information is rich relatively and the gradient magnitude distribution is scattered, the value of σ will be larger, in order to keep more edge information, the value of k should be smaller. Otherwise, the value of σ is smaller, and the value of k is bigger.

2. Method for image with rich edge information

In images with a large field of view, rich edge information and scattered gradient magnitude distribution, the contrast of each part of the entire image is inconsistent, and the image gradient's standard deviation is large relatively. Selecting a double-threshold for the whole image can not help accomplish edge detection, since the selected threshold will be too high for some edge regions with small gradient magnitude, which will lead to the loss of detail edges. For this kind of images, this paper proposed a method to select a double-threshold for each pixel. Firstly, the mean of gradient magnitude of the whole image E_{ave} is calculated by (21). If the gradient magnitude of pixel $I[i, j]$ is smaller than 15% ~ 20% of the E_{ave} , it will be marked as non-edge point directly. This process contributes to guarantee that for image with large field of view and rich edge information, the improved algorithm won't introduce more noise in areas where there are few edges, that is, the mean of gradient magnitude and standard deviation of these areas are very small. The threshold for pixel $I[i, j]$ is calculated based on the mean of the gradient magnitude and standard deviation of the elements in the $N \times N$ matrix image gradient, whose center is the pixel $I[i, j]$ (N is an odd number, generally larger than (20)). Then, the threshold value of the pixel can be obtained by (23). When the pixel $I[i, j]$ is located in the border area of the image and the matrix is less than $N \times N$, the insufficient parts were set null, then calculate the mean and standard deviation of this matrix to obtain the threshold. Therefore, every pixel has its corresponding double-threshold, and the whole image's edge information can be obtained through detecting and connecting edges.

3. Methodology

In this work, two different methods of defining edges (Sobel and improve canny edge detection) will be applied to the dataset obtained from micro-bubbles, and these two methods are compared in terms of results. The figure below shows the mechanism of work.



Figure 1: general proposal system

3.1. Microbubbles Dataset

Images of ellipse-shaped bubbles with particular geometric center coordinates, as well as values assigned to axle suspensions and a semi-major rotation angle. For the natural flow direction of bubbles. Monomorphic randomness is used to generate a position engineering center from bubbles. Regular distributions are used to create corresponding semi-axial volumes and angles of rotation values. As a result, the whole generated image space is used to place bubbles. Situations outside the present image, in the middle of a bubble, are simulated. The distribution of physically meaningful density from the edge of the bubble is added to the black background and imposed with gaussian noise and particle images, which are created with specific programs that take into account different physical conditions such as lasers, simulating the distribution of brightness of bubble image density. For medium air and water, calculations are done. At a 6060 pixel interval, the average brightness is computed. The bubble's edge, as seen in the graph, reaches its brightest point at a distance of roughly 70% of its true radius. To improve the resemblance to actual data, 200 square images of the backdrop were obtained from the original data without bubbles. These images are utilized as random masks in the examples generated, using a double process sampled at intervals of $[0.01, 0.5]$ for each image generated as shown in Figure (2).

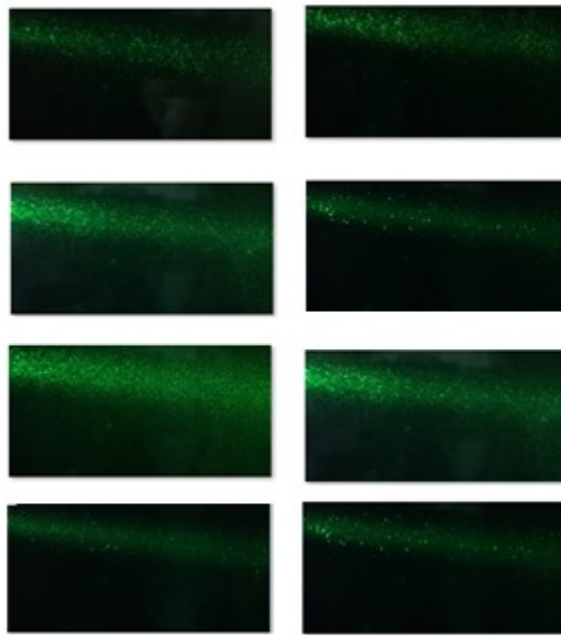


Figure 2: Samples of Microbubbles Dataset

3.2. Pre-processing stage

It is well known that the most important image processing operations will not start unless pre-processing is performed first. Its goal is to refine the target image to obtain better results in further processing. The preprocessing operations performed on the models at this point are as follows: Convert the image from RGB to the HSV store in the database.

Step1: Calculate the RGB three-band value, then convert to HSV space.

Step2: Biggest of $(R., G., B.)$ must be found; $\text{Max}(R, G, B)$.

Step3: Smallest of $(R., G., B.)$, must be found; $\text{Min}(R., G., B.)$.

Step4: Find Δ by the difference between M_{max} , M_{min} .

Step5: a Compute (hue, H) value, where $H = G - B/\Delta$ and $H = 2 + (B - R/\Delta)$ and $H = 4 + (G - B/\Delta)$.

Step6: Compute the brightness, V value ($V = M_{\text{max}}$).

Step7: Compute the saturation, S value ($S = \Delta/V$).

3.3. Improved Canny Edge Detection Stage

To highlight and extract small bubbles, it is necessary to utilize a method to extract the edges of the bubble, provided they maintain their accuracy, and also because the bubbles are thin and not thick, so we utilized canny edge detection due to the amount of data in the image and the ability of this method to maintain the structural properties of image processing and the When it comes to detecting horizontal and vertical edges, the clever edge detector performs admirably. It's also capable of detecting circular and corner edges. Detecting edges facilitates the ability to determine the detection of the sharp edge of a small bubble image. The canny algorithm's effectiveness is largely reliant on changeable parameters like Sigma, the standard deviation of Gaussian filtering, and threshold values like "TH" and "TL." The size of the Gaussian filter is likewise controlled by Sigma. The larger the Gaussian filter size, the higher the value of the. This causes more fuzzy images, which is essential for noisy photos, as well as bigger edge detection. However, as predicted, the larger the Gaussians are, the less accurate the edge leveling becomes. Narrower numbers indicate a smaller Gaussian filter, which reduces blur while preserving sharper image edges. By adjusting these changeable parameters, the user can alter the algorithm. The outcome will be different if the sigma value and mask are modified, according to the analysis. The image quality is poor for such a high value from Sigma, since it creates points with a broad range of values. As a result, finding accurate margins becomes harder. The execution time increases when you use a higher value from the mask. This algorithm can provide results that are more suitable for tiny bubbles by setting the right value to these parameters. Algorithm below presents the applied steps for improved canny edge detection.

Step 1: Read *HSV* image

Step2: Gaussian Filter Coefficient Convolution

Step3: Horizontal and vertical orientation convolution using Canny Filter.

Step4: Using atan2 to calculate directions

Step5: Adjusting to the closest (0, 45, 90 , 135) degree

Step6: aNon-Maximum Suppression

Step7: Hysteresis Thresholding using two values for Thresholding, T_{High} , and T_{Low}

4. Experimental results

In this paragraph, the results obtained are explained as shown below.

4.1. Preprocessing Stage

In preprocessing stage, a two-color model is used (HSV and YCbCr). HSV model is shown more effective than YCbCr model because the appearance of microbubbles more clear is shown than YCbCr. Figure (3) and Figure (4) are plotting with their histogram and can be noticed the difference between two color space models in resulted Microbubbles image.

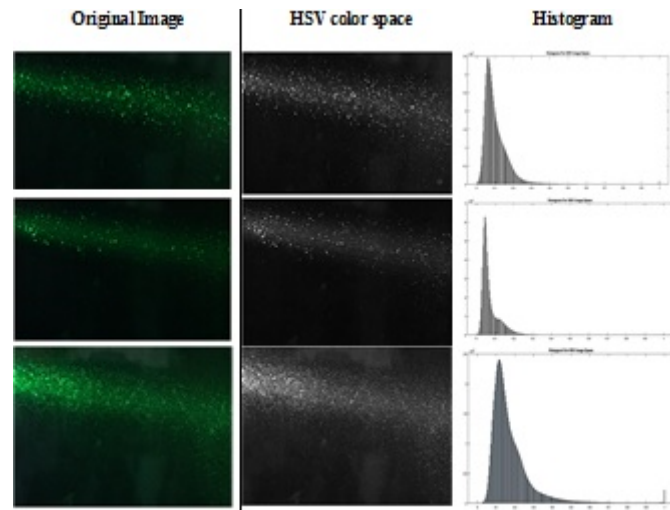


Figure 3: Sample of *HSV* Color Space with their Histogram

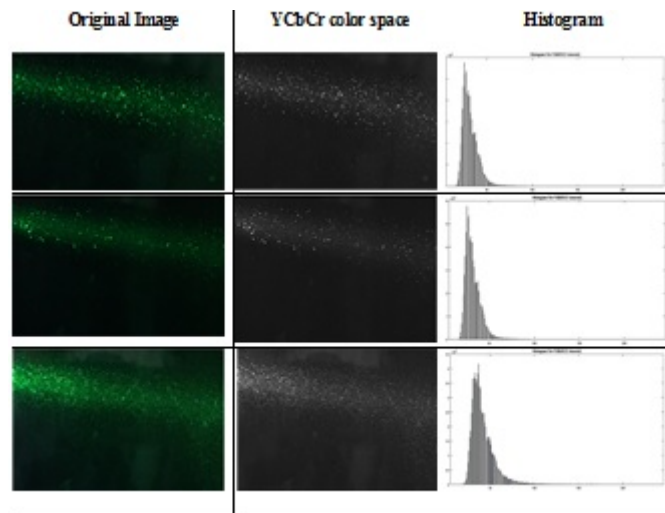


Figure 4: Sample of *YCbCr* Color Space with their Histogram

4.2. Edge Detection

Edge detection is the next stage of our proposed system. In this stage, two different operations are used.

4.2.1. Improved Canny Edge Detection

Edge detection reduces the quantity of data in a image while preserving the structural characteristics for further image processing as shown in Figure (5). In this case, the strong edges can be found by using the improved canny edge detection method by taking angle each angle takes sigma, and kernels were used to set a parameter that is open every time can be changed to give better results by work. The best parameter of kernels (x, y) when sigma =2, and threshold value =0.3.

4.2.2. Sobel Operation

To have the confusion matrix evolve, all of the stages of the CNN stated in Chapter three must be utilized; just modify the input parameters to CNN and make them suitable for the process of

evolution, depending on the CNN, confusion matrix computation, Figure (6) depicts a plot with rows and columns and diagonal cells for a confusion matrix, where predicted class represents rows, which is the (Output Class), and true class represent columns, which is the (Target Class), and the percentage represents how many or how much the trained network has learned.

4.2.3. Comparison between Canny and Sobel operation

In the Sobel as against Canny comparison, we find that the Canny edge detector can detect the most edges for microbubbles. In the Canny vs. Sobel comparison, we observe that the Canny edge detector can detect the most edges for microbubbles. Canny’s edge detector detects horizontal and vertical edges well for microbubbles. Canny’s edge detector performs well at detecting horizontal and vertical edges. It can identify circular and corner edges as well. Sobel does a good job at recognizing horizontal and vertical edges. In compared to the Canny, Sobel provides low-quality edge maps, as seen by the microbubbles image. The Canny approach is one of the Sobel techniques that can detect both strong and weak edges. The canny method’s performance is primarily determined by the variable parameters Sigma, which is the Gaussian filter’s standard deviation, and high and low threshold values. The Gaussian filter size is likewise determined by Sigma. The size of the Gaussian filter increases as increases value. This means increased blurring, which is necessary for images of noise, And so on the ability to recognize bigger edges. However, as expected, Gaussian’s scale large, the less accurate edge localization becomes. Smaller numbers imply a smaller Gaussian filter, reducing blurring and preserving the image’s finer edges. By adjusting these changeable parameters, the user may fine-tune the algorithm. Following more study, it was discovered that altering the sigma and mask values yielded a different outcome. The image quality is poor with a big sigma value because it creates points that are scattered throughout a wide range of values. As a result, finding precise margins becomes harder. The execution time increases when the mask value is raised. As a consequence, by adjusting the values of these parameters, this algorithm can produce more appropriate results,as shown in Figures (5) and (6).

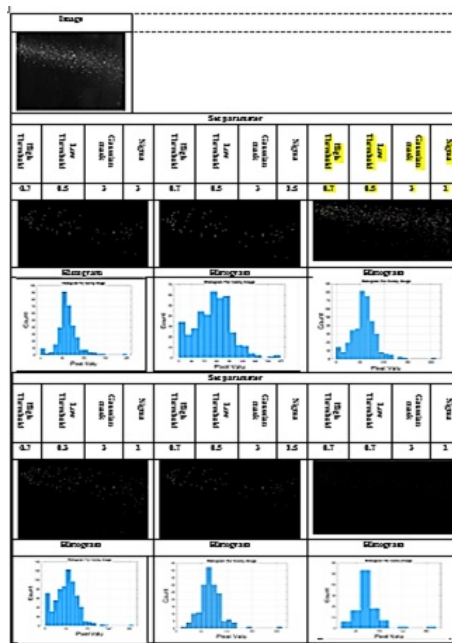


Figure 5: improved canny edge detection

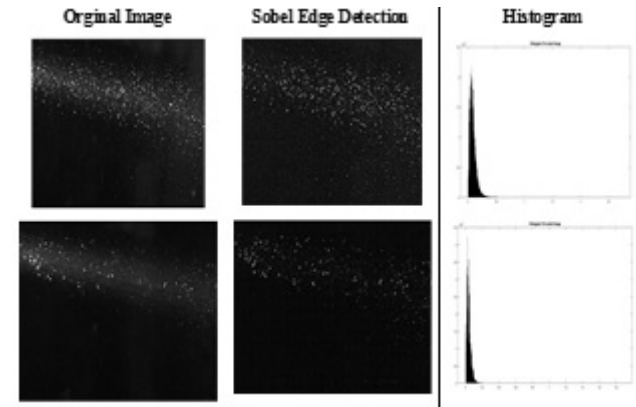


Figure 6: Sobel edge detection

5. Conclusion

One of the major contributions to this work was the creation of a new standard for classifying microscopic bubbles. One of the problems was in creating the data set and extracting the small bubbles and making sure that all the included images were taken using the same environmental conditions, such as lighting, and only the bubbles that were 20 to 50 microns in size were taken, equivalent to 4 pixels to 8 pixels. To solve these problems, an improvement technique has been applied that includes the use of a set of methods described below. Several Conclusions can be stated from the achieved results, which are summarized as follows where Two enhancement methods are used that are based on the YCbCr and HSV color space. Evidence from this study indicates the idea of using HSV-based image enhancement technology during the pretreatment stage to classify microbubbles as more appropriate because it preserves the bubble color value through which data is not lost and dark bubbles are less and we notice the difference in Figure (3) and (4). For the stage of determining the edges of the microbubbles and highlighting them on the basis of Sobel operation, it is indicated that using it gives good results because it preserves the edges of the bubble, unlike other methods When using canny edge detection, the microbubbles have disappeared, because the first stage in it was used As for the stage of defining the edges of the microbubbles and highlighting them based on the canny edge detection, it is indicated that its use gives good results because it preserves the edges of the bubble, whether it is weak or strong, and this sharp edges because it was taken at different angles, and also the number of bubbles extracted is real because one of the steps is used Gaussian filter, which in turn performs the Blurring process of the image, thus, the bubble in its turn is thinner and remove noise and Fake bubbles .Unlike the Sobel method, when using it, we note that all the edges of the bubbles are extracted, and it is possible that some of them are fake and inaccurate, despite the huge number that you extract from minute bubbles. we notice the difference in the Figure (5) and (6).

References

- [1] S. Agaian, A. Almuntashri and A.T. Papagiannakis, *An improved Canny edge detection application for Asphalt concrete*, Proc. 2009 IEEE Int. Conf. Systems, Man, and Cybernetics USA, 2009 pp.3683–3687.
- [2] R. C. Bueno, P.H.F. Masotti, J.F. Justo, D.A. Andrade, M.S. Rocha, W.M. Torres and R.N.de Mesquita, *Two-phase flow bubble detection method applied to natural circulation system using fuzzy image processing*, Nuclear Engin. Design 335 (2018) 255-264.
- [3] J. Canny, *A computational approach to edge detection*, IEEE Trans. Pattern Anal. Machine Intell. 8 (1986) 679–698.
- [4] R. Gonzalez and R. Woods, *Digital Image Processing*, Addison Wesley, 1992.

-
- [5] Li Er-sen, Zhu Shu-long, Zhu Bao-shan, Zhao Yong, Xia Chao-gui and Song Li-hua, *An adaptive edge-detection method based on the Canny operator*, Int. Conf. Envir. Sci. Inf. Appl. Tech. (2009) pp.465–469.
 - [6] C. Lopez-Molina, H. Bustince, J. Fernandez, P. Couto and B. De Baets, *A gravitational approach to edge detection based on triangular norms*, Pattern Recogn. 43 (2010) 3730–3741.
 - [7] Mitani, Yoshihiro and O. Toshitaka, *Detection of microbubbles using the Hough transform*, Applied Mechanics and Materials, 378 (2013) .
 - [8] T.B. Nguyen and D. Ziou, *Contextual and non-contextual performance evaluation of edge detectors*, Pattern Recogn. Lett. 21 (2000) 805–816.
 - [9] F.A. Pellegrino, *Edge Detection Revisited*, IEEE Trans On System Man and Cybernetics, 34 (2004) 1500–1517.
 - [10] S. Sara and H. jamela, *Edge Detection of Ear Image Based on Canny Method*, The 23rd Specialized Scientific Conference, collage of Education / University Mustansiriya 26-27 April 2017.
 - [11] S. Salman and H. Jamila, *Deep learning machine using Hierarchical cluster features*, Al-Mustansiriyah J. Sci. 29 (2019) 82–93.
 - [12] M. William, *The Canny Edge Detector Revisited*, Int. J. Computer Vision 91 (2011) 251–261.
 - [13] Y.J. Zhang, *Image Engineering(II)Image Ananlysis*, Tsinghua University press, Beijing, 2007.
 - [14] Q. Zhao, R.-R. Li and Q. QU, *Research on statistical detection method of micro bubbles in transparent layer of quartz crucible based on image processing*, J. Crystal Growth 556 (2020).